BIOCHEMISTRY
including biophysical chemistry & molecular biology

ARTICLE

pubs.acs.org/biochemistry

Protein Interactions among Fe65, the Low-Density Lipoprotein Receptor-Related Protein, and the Amyloid Precursor Protein

Melinda M. Mulvihill, Miklos Guttman,[†] and Elizabeth A. Komives*

Department of Chemistry and Biochemistry, University of California, San Diego, La Jolla, California 92093-0378, United States

Supporting Information

ABSTRACT: The adapter protein Fe65 has been proposed to be the link between the intracellular domains of the amyloid precursor protein, APP (AICD), and the low-density lipoprotein receptor-related protein (LRP-CT). Functional linkage between these two proteins has been established, and mutations within LRP-CT affect the amount of Aβ produced from APP. Previous work showed that AICD binds to protein interaction domain 2 (PID2) of Fe65. Although the structure of PID1 was determined recently, all attempts to demonstrate LRP-CT binding to this domain failed. We used biophysical experiments and binding studies to investigate the binding among these three proteins. Full-length Fe65 bound more weakly to AICD than did N-terminally truncated forms; however, the intramolecular domain−domain interactions that had been proposed to inhibit binding could not be observed using amide H−D exchange. Surprisingly, when LRP-CT is phosphorylated at Tyr4507, it bound to Fe65 PID1 despite the fact that this domain belongs to the Dab-like subclass of PIDs that are not supposed to be phosphorylation-dependent. Mutation of a critical arginine abolished binding, providing further proof of the phosphorylation dependence. Fe65 PID1 thus provides a link between the Dab-like class and the IRS-like class of PIDs and is the first Dab-like family member to show phosphorylation-dependent binding.

The β-amyloid precursor protein (APP) is a type I membrane protein that can be processed to β-amyloid (Aβ), the main component of amyloid plaques in Alzheimer's disease (AD). The complicated processes that lead to Aβ production are not well understood. Processing of APP is affected by the expression levels of both the low-density lipoprotein receptor-related protein (LRP) and Fe65.[1−7] The APP intracellular domain (AICD) contains an NPXY motif at positions 684−687, a motif known to interact with protein interaction domains (PIDs, also known as phosphotyrosine binding domains or PTBs).[8] Crystal structures of AICD interacting with PIDs,[9,10] including the C-terminal PID of Fe65,[11] have been determined.

LRP is an endocytic receptor composed of a 515 kDa α-subunit and an 85 kDa β-subunit that are noncovalently associated. The intracellular domain of LRP (LRP-CT) contains two NPXY motifs at positions 4470−4473 and 4504−4507 that can both be phosphorylated.[12,13] LRP expression levels have been shown to affect Aβ production.[1,5] Pietrzik et al. showed the C-terminal region of LRP, in particular the second NPXY motif, was responsible for LRP's effect on Aβ production.[3] Furthermore, mutation of the tyrosine in this motif abolished these effects.

Fe65 is a 97 kDa adapter protein that contains a WW domain followed by two PIDs. Like LRP-CT, Fe65 expression levels have been shown to affect Aβ production.[2,4,6,7] In most studies, an increased level of Fe65 expression resulted in a decreased level of Aβ production. Fe65 can also be linked to AD through a splice variant, Fe65a2. This isoform has an altered C-terminus and showed resistance to very late onset Alzheimer's disease, possibly through weakened binding to APP.[14] The C-terminal PID (PID2) of Fe65 interacts with AICD,[11,15,16] and the crystal structure of this complex reveals a unique binding interface that is much larger than those of other known PID interactions.[11] AICD in which the tyrosine in the NPXY motif was mutated to alanine (Y687A) retained the ability to bind Fe65.[16] Both the structure and mutational analysis suggest that PID2 can bind AICD in both the tyrosine-phosphorylated (NPXpY) and nonphosphorylated forms, but the Fe65−AICD NPXpY interaction has not yet been observed.

Fe65 can be processed to a 65 kDa form lacking the N-terminal region, and this shorter form was shown qualitatively to have enhanced binding to AICD, leading to speculation that intramolecular domain interactions may be present in Fe65.[17] Intramolecular interactions were also proposed on the basis of observations of WW domain−PID2 binding in solution.[18] One goal of the work presented here was to probe these intramolecular interactions and quantify their effect on binding affinity.

The N-terminal PID (PID1) of Fe65 has been reported to interact with the histone acetyltransferase Tip60, transcription factor CP2, the cytoplasmic domain of the ApoER2 receptor, and LRP-CT.[7,19−21] Interestingly, neither CP2 nor Tip60 contains an NPXY motif. The intracellular domain of ApoER2 does contain an NPXY motif and was shown by co-IP to interact with Fe65 constructs containing PID1 in COS7 cells.[7] The Fe65−LRP interaction has been shown in numerous in vivo assays. GST-Fe65 PID1 was able to pull down LRP-CT in MEF cells.[19] In a later study, FRET

Received: April 4, 2011
Revised: June 7, 2011
Published: June 08, 2011

was observed between Fe65 PID1 and LRP-CT in an H4 cell line.[22] Lastly, co-IP experiments detected Fe65−LRP-CT complexes in HEK293T cells. This interaction could be observed with LRP-CT in which either NPXY motif was deleted, but binding was not observed when both NPXY motifs were deleted.[23] The single in vitro experiment showing Fe65 binding to LRP-CT was performed by exploiting the trimeric interaction of GST LRP-CT, Fe65, and APP695. A GST LRP-CT pull-down assay of Fe65 was confirmed by detection of APP ^{35}S.[23] Radzimanowski et al. were unable to confirm binding of Fe65 PID1 to Tip60, ApoER2, or LRP-CT by isothermal titration calorimetry (ITC), regardless of the phosphorylation state of the NPXY motifs. In vitro binding assays using purified proteins are needed to show direct Fe65 PID1 interactions and the effect the NPXY tyrosine phosphorylation state has on binding.

Protein interaction domains (PIDs) were formerly called phosphotyrosine binding domains (PTB), but because phosphorylation is not a binding requirement in all cases, the domain was renamed. PIDs can be divided into three families based on structural similarities and binding modes: IRS-like, Shc-like, and Dab-like.[24] IRS-like PIDs use two arginine residues to coordinate the phosphate moiety in the NPXpY motif. Shc-like PIDs use two arginine residues and a lysine residue to coordinate the phosphate. Dab-like PID binding events are not phosphorylation-dependent. Both PIDs in Fe65 have been classified as Dab-like PIDs. Although PID1 has been classified as a Dab-like PID, it contains two key arginine residues that overlap with the IRS binding pocket arginines in structural and sequence alignments.[25,26] These arginines could coordinate a phosphate moiety, although binding of a phosphorylated ligand to PID1 has not been observed.

Using a combination of biophysical experiments and binding assays on purified proteins, we provide evidence of the Fe65 PIDs binding to the NPXY motifs in LRP-CT and AICD. Surprisingly, Fe65 PID1 binds the LRP-CT $NPXY_{4507}$ motif only when it is tyrosine-phosphorylated. LRP-CT forms a trimeric complex with Fe65 and AICD only when this LRP-CT $NPXY_{4507}$ motif is tyrosine-phosphorylated. Fe65 PID1 is therefore the first example of a Dab-like PID that binds an NPXY motif in a phosphorylation-dependent manner.

MATERIALS AND METHODS

Protein Expression and Purification. Human Fe65 constructs containing PID2 (residues 1−662, 236−662, 534−662, or 1−708) were expressed with a N-terminal ubiquitin tag to aid in solubility. The ubiquitin fusion vector was generated by cloning the DNA sequence for human ubquitin into the NcoI and BamH1 sites of pHis8.[27] Fe65 proteins were expressed in BL21(DE3) cells and induced with 0.2 mM IPTG overnight at 18 °C in M9ZN medium (M9 medium supplemented with 10 g/L NZ amine). The cell pellet was resuspended in TBS lysis buffer [50 mM Tris-HCl (pH 8), 500 mM NaCl, 1 mM BME, and 0.5 mM PMSF], sonicated on ice, and centrifuged for 40 min at 12000 rpm. Soluble proteins were captured using Ni-NTA (Qiagen) in TBS (pH 8.0) at 4 °C, eluted with 250 mM imidazole, and further purified on a Superdex-75 or Superdex-200 gel filtration column (GE Healthcare) in 50 mM Tris-HCl (pH 8), 150 mM NaCl, 1 mM DTT, and 1 mM EDTA. The eluted protein was concentrated in a 10 kDa molecular mass cutoff Amicon Ultra centrifugal filter (Millipore).

The APP intracellular domain (AICD, residues 649−695 using APP695 numbering) with an N-terminal cysteine was cloned into the pMMHb vector modified to include an additional thrombin cleavage site after the TrpLE peptide.[27] AICD was expressed in BL21(DE3) cells and induced with 1 mM IPTG for 4 h at 37 °C. The cell pellet was resuspended in lysis buffer, sonicated on ice, and centrifuged for 40 min at 12000 rpm. After resolubilization of inclusion bodies by sonication in 8 M urea TBS (pH 8), protein was loaded onto a 5 mL pre-equilibrated NTA-Ni column. The resulting slurry was washed with 8 M urea TBS (pH 8) followed by thrombin cleavage buffer [2 mM $CaCl_2$ TBS (pH 8)]. The slurry was then incubated with 25 ng of thrombin in 20 mL of cleavage buffer overnight at 25 °C. Cleaved protein was washed from the column and purified by reverse phase high-performance liquid chromatography (RP-HPLC). The resulting AICD was lyophilized and stored at −20 °C.

The human LRP1 gene fragment containing the cytoplasmic domain as well as six residues of the membrane-spanning region (residues 4439−4544) was subcloned into PGEX-4T2. GST fusion proteins were expressed in pLysS cells and induced with 0.2 mM IPTG overnight at 18 °C in M9ZN medium. The cell pellet was resuspended in lysis buffer, sonicated on ice, and centrifuged for 40 min at 12000 rpm. The supernatant was loaded on a 10 mL pre-equilibrated glutathione Sepharose column at 4 °C, washed with 3 column volumes of TBS, and eluted in 10 mL of 10 mM glutathione in TBS (pH 7.4). The eluted protein was concentrated in a 10 kDa molecular mass cutoff Amicon Ultra centrifugal filter (Millipore) and loaded onto a Superdex-75 gel filtration column in 50 mM Tris-HCl (pH 7.4), 150 mM NaCl, and 1 mM DTT. AICD Y653F, Fe65 R451Q, and LRP-CT Y4478F mutations were introduced using QuickChange mutagenesis (Strategene, La Jolla, CA) and verified by DNA sequencing. Protein concentrations were determined by UV absorbance, and identities were confirmed by matrix-assisted laser desorption ionization time-of-flight (MALDI-TOF) mass spectrometry.

LRP microdomains containing Tyr4507 (Cys-amino aminohexanoic acid-TNFTNPVY$_{4507}$ATLY) and Tyr4473 (Cys-amino aminohexanoic acid-VEIGNPTY$_{4473}$KMYEGGE) in both phosphorylated and nonphosphorylated forms were prepared as described previously.[28]

LRP4488 contains residues 4488−4544 of human LRP1 with an N-terminal cysteine and was cloned into the pMMHb vector modified to include an additional thrombin cleavage site after the TrpLE peptide.[27] Expression was conducted as described for AICD.

Phosphorylation of LRP-CT Y4478F, AICD Y653F, and LRP4488. Chicken Src (residues 251−533) was expressed and purified according to previously published protocols.[29] Tyrosines in LRP, Y4478F, and AICD, Y653F, were mutated to ensure exclusive phosphorylation of GST-LRP-CT at Y4507 and AICD at Y687. GST-LRP-CT, AICD, or LRP4488 (230 nmol) was incubated with 0.7 nmol of purified recombinant c-Src in 2 mL of 1 mM ATP, 100 mM $MnCl_2$, 100 mM $MgCl_2$, and TBS (pH 7.4) for 1 h at 25 °C.

SPR Binding Experiments. Sensorgrams were recorded on a Biacore 3000 instrument using streptavidin chips as described previously.[30] AICD was biotinylated at the N-terminal cysteine using biotin-maleimide (Pierce); 100, 200, and 300 RU of AICD were immobilized, and 50−500 nM Fe65 was injected for 5 min and dissociation assessed for 20 min at 25 °C at a flow rate of 50 μL/min. No regeneration step was necessary. Data were fit using BiaEvaluation version 2.0 and plotted in Origin 7.0.

Amide Exchange Experiments. Native state backbone amide exchange was measured as described previously. Fe65 with or without a 2-fold excess of AICD was incubated for 0−10 min in deuterated TBS buffer (pH 8). Amide exchange was quenched by 10-fold dilution into ice-cold 0.1% TFA until the final pH was 2.2.

The sample was immediately digested with an excess of immobilized pepsin (Pierce), and the digest mixture was frozen in liquid N_2. All samples were analyzed on the same day by MALDI-TOF mass spectrometry.[31] The centroids of the mass envelopes were measured and compared to undeuterated controls and corrected for back exchange as described previously.[32]

Pull-Down Assays. AICD and LRP-CT microdomains were immobilized using a Sulfolink coupling gel according to the manufacturer's directions (Pierce, Rockford, IL). Because of the poor solubility of the peptides, all Sulfolink immobilization reactions were conducted in 3.5 M guanidine hydrochloride with TBS (pH 8.0). The amount of peptide immobilized was quantified by UV absorbance. The efficiency of immobilization was found to be 1−2 mg of peptide/mL of beads.

Equal amounts of GST-LRP-CT or GST-LRP-CT (pY4507) were immobilized on glutathione Sepharose beads at 1 mg/mL (50% slurry) for 1 h at 4 °C in 50 mM Tris-HCl (pH 7.4), 150 mM NaCl, and 1 mM DTT. The resulting resin was washed four times in TBS-X [50 mM Tris-HCl (pH 7.4), 150 mM NaCl, 1 mM DTT, 2 mM $CaCl_2$, 2 mM $MgCl_2$, and 1% Triton X-100] before being used as bait for Fe65 binding reactions.

Binding reactions were conducted in 1 mL of TBS-X containing 15 μL (for AICD and LRP microdomains) or 25 μL (GST-LRP-CT) of washed beads and 55 nM to 1.2 μM Fe65. Trimeric binding reaction mixtures contained 5 μM immobilized AICD, 2.5 μM Fe65, and 260 nM GST-LRP-CT. Fe65 PID2 competition binding reaction mixtures contained 650 μM GST LRP-CT, 650 μM AICD, and 24 μM Fe65 PID2 (536−662). Reaction mixtures were incubated at 4 °C for 1−2 h, washed four times in TBS-X, and resuspended in 30 μL of reducing SDS buffer. Samples were resolved by sodium dodecyl sulfate−polyacrylamide gel electrophoresis, transferred to a PDVF membrane, and probed with the Fe65 antibody (1:500, Millipore, 3H6), LRP antibody (1:500, 11H4), anti-HIS antibody (1:1000, Qiagen, Penta-His Ab), or anti-ubiquitin antibody (1:100, Invitrogen 13-1600). The 11H4 anti-LRP antibody was a generous gift from P. van der Geer.

LRP4488 Labeling for Fluorescence Anisotropy Experiments. LRP4488 or LRP4488 phosphorylated at Y4507 (pYLRP4488) was labeled with Oregon Green 488 maleimide (Invitrogen, O-6034) at the single cysteine introduced at the N-terminus according to the manufacturer's instructions. One milliliter of 100 μM LRP4488 or pYLRP4488 was reduced with immobilized TCEP (Pierce) for 1 h in TBS (pH 7.5) at room temperature. Reduced LRP4488 was incubated with a 20-fold excess of Oregon Green 488 and allowed to react for 2 h at room temperature in the absence of light. The labeled LRP4488 or pYLRP4488 was purified by RP-HPLC and lyophilized.

Fluorescence Anisotropy Experiments. Polarization experiments were performed with 96-well black fluorescence plates (Fluotrac, Greiner Bio-One) on a DTX 880 Multimode Detector Beckman Coulter plate reader with an excitation filter at 485 nm and two emission filters at 535 nm equipped with polarizers. Fe65 (0.1−100 μM) with and without 20 nM LRP4488 or pYLRP4488 in 50 mM Tris-HCl (pH 7.5), 150 mM NaCl, and 1 mM DTT was added to the wells, and the plates were incubated for 30 min before readings were taken. Anisotropy values at each concentration were determined after subtracting the intensities for Fe65 alone, using the equation $r = [I_{(V,V)} - GI_{(V,H)}]/[I_{(V,V)} - 2GI_{(V,H)}]$, where r is the anisotropy, $I_{(V,V)}$ is the fluorescence intensity in the parallel direction, $I_{(V,H)}$ is the fluorescence intensity in the perpendicular direction, and G is 0.67, a correction factor for the difference in detection sensitivity for parallel and perpendicular polarized light. Data were fit with KaleidaGraph 4.0 using the Michaelis−Menten curve fit.

RESULTS

The N-Terminal Domains of Fe65 Weaken Binding of Fe65 PID2 to AICD. Surface plasmon resonance (SPR) binding experiments were performed with AICD (residues 649−695 of the β-amyloid precursor protein) and various Fe65 constructs to explore the inhibitory effects of the N-terminus of Fe65 on the binding of Fe65 PID2 to AICD. Fe65 constructs containing PID2 are unstable in solution and highly prone to aggregation. A ubiquitin tag was introduced to aid solubility and effectively alleviated these problems. Ubiquitin-Fe65 was able to interact with AICD with affinities similar to those reported in the literature.[11] Fe65 containing the full N-terminus (residues 1−662) bound AICD 2.5-fold weaker (K_D = 2.54 ± 0.35 μM) than Fe65 lacking the N-terminus (residues 236−662) (K_D = 1.01 ± 0.05 μM) (Figure 1A,B). Further truncation of Fe65 to a construct containing only PID2 (534−662) enhanced binding an additional 3-fold (K_D = 0.35 ± 0.02 μM) (Figure 1C). These results indicate the N-terminal domains do in fact have an inhibitory effect on AICD binding. The N-terminal domains primarily slow the association rate (Table 1).

To probe for Fe65 intramolecular interactions, we compared the amide hydrogen−deuterium (H−D) exchange behavior of Fe65 (1−662) and Fe65 (236−662). Peptic fragments covered 44% of PID2 (residues 534−662), including regions of the Fe65 AICD binding interface. H−D exchange analysis showed identical exchange with or without the presence of the 235 N-terminal amino acids. Representative plots are shown in Figure 2A,B (Fe65 1−662 (●), Fe65 236−662 (■)) and the data from the 5 min time point for all peptides from PID2 are summarized in Table 2A. The deuterons incorporated into the region of residues 638−649 could not be quantitatively determined because of spectral overlap but qualitatively showed the same exchange with and without the N-terminal region. To ensure that protein interactions would lead to observable changes in H−D exchange, the same experiment was performed with Fe65 (236−662) in the presence of AICD. Significant changes at the AICD binding interface in PID2 were clearly evident [Figure 2B (◆)].

A second Fe65 intramolecular interaction has been proposed in which the WW domain interacts with PID2.[18] Amide H−D exchange of Fe65 with and without PID2 (residues 236−662 vs residues 236−512) showed no changes in the WW domain (residues 253−289, with 81% coverage). Representative plots are shown in Figure 2C,D, and the data from the 5 min time point for all peptides from the WW domain are summarized in Table 2B. The results show no evidence of any strong Fe65 intramolecular interaction involving the WW domain or PID2.

Fe65 Can Bind AICD Phosphorylated at the Tyrosine in the $NPXY_{687}$ Motif. PID2 of Fe65 has been classified as a Dab-like PID, the category of PIDs reserved for those that bind nonphosphorylated ligands.[24] Dab-like PIDs in some cases strongly disfavor tyrosine phosphorylation, and in some cases, phosphorylation does not affect binding. Fe65 PID2 has not been shown to directly bind any ligand in the NPXpY form. The binding interface of PID2 and AICD is unique in that it is 3 times larger than those of known PID peptide interactions.[11] We sought to determine if Fe65 could bind APP phosphorylated at the tyrosine in the $NPXY_{687}$ motif. Phosphorylation reactions with purified recombinant Src and AICD resulted in AICD

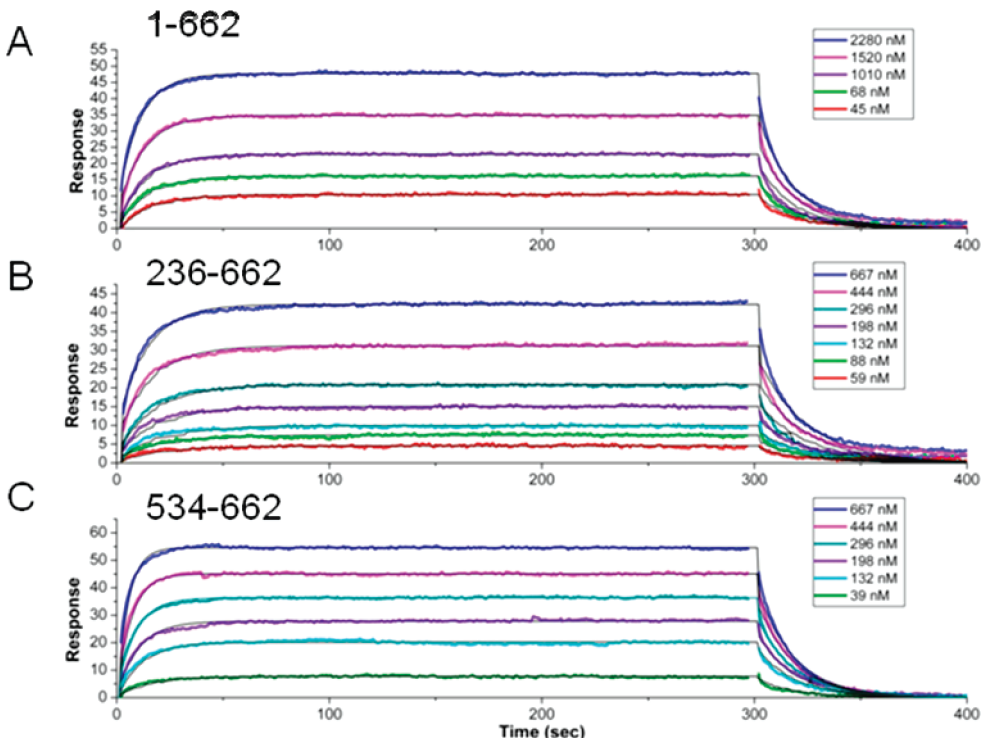

Figure 1. SPR binding kinetics of the interaction between AICD and Fe65 N-term-WW-PID1-PID2 (1−662) (A), Fe65 WW-PID1-PID2 (236−662) (B), or Fe65 PID2 (534−662) (C) performed as previously described.[30] AICD was biotinylated at the N-terminus through an engineered cysteine and immobilized on a streptavidin sensor chip. Fe65 (50−500 nM) was the flowing analyte. The data were collected on a Biacore 3000 and fit using a simple 1:1 binding model yielding for a K_D of 2.54 ± 0.35 μM for Fe65 (1−662), a K_D of 1.01 ± 0.05 μM for for Fe65 (236−662), and a K_D of 0.35 ± 0.02 μM for Fe65 (534−662).

Table 1. SPR Results for the Various Fe65 Constructs Binding to AICD

Fe65 construct	K_D (μM)	k_a (M^{-1} s^{-1})	k_d (s^{-1})	X^2
1−662	2.5 ± 0.35	2.2×10^4	0.055	0.78
236−662	1.0 ± 0.05	5.7×10^4	0.057	0.22
534−662	0.35 ± 0.02	9.5×10^4	0.033	0.432

phosphorylation at Y653 and Y687. AICD Y653F was used to ensure phosphorylation exclusively at Y687. AICD or AICD-pY_{687} was coupled to Sulfolink resin through an N-terminal cysteine and incubated with Fe65 (236−662). Fe65 binds AICD and AICDpY_{687} equally well (Figure 3), showing that PID2 of Fe65 can bind ligands in both the phosphorylated and nonphosphorylated states.

Tyrosine-Phosphorylated and Nonphosphorylated LRP-CT NPXY$_{4507}$ Microdomains Bind Distinct Domains in Fe65. LRP-CT contains two NPXY motifs (residues 4470−4473 and 4504−4507) that can both be phosphorylated.[13,33] The phosphorylation state preference of the Fe65 PIDs binding to the LRP NPXY motifs has not been fully explored. Using microdomains centered at each LRP NPXY motif, we investigated the specificity of Fe65 PID binding to each LRP NPXY motif in the tyrosine-phosphorylated and nonphosphorylated forms. Each microdomain peptide was coupled to Sulfolink resin and incubated with Fe65 WW-PID1-PID2 (236−662), Fe65 WW-PID1 (236−512), or Fe65 PID2 (536−662). All experiments were conducted with freshly prepared, pure Fe65 proteins (Figure 1 of the Supporting Information). The LRP microdomains containing Y4473 showed no interaction with Fe65 regardless of their phosphorylation state (Figure 4A, lanes 3 and 4). On the other hand, microdomains containing Y4507 bound Fe65 in both the phosphorylated and nonphosphorylated forms (Figure 4A, lanes 5 and 6). The same assay with Fe65 (236−512) and Fe65 PID2 (536−662) suggests that PID1 interacts with phosphorylated Y4507 while PID2 interacts with the nonphosphorylated Y4507 (Figure 4B,C, lanes 5 and 6).

Recapitulation of the Observed FE65 Binding Preferences in Full-Length LRP-CT. To determine if the specificity of Fe65 PID1 for LRP-CT in the Y4507-phosphorylated form and Fe65 PID2 for the nonphosphorylated form was also observed in the context of full-length LRP-CT, we prepared GST-LRP-CT Y4473F phosphorylated exclusively at Y4507 with recombinant purified Src. GST-LRP-CT (pY4507) or nonphosphorylated GST-LRP-CT was immobilized on glutathione Sepharose and incubated with purified Fe65 constructs (Figure 5). In agreement with the LRP microdomain results, Fe65 WW-PID1-PID2 bound both GST-LRP-CT (pY4507) and nonphosphorylated GST-LRP-CT. Fe65 in which one of the arginines conserved in PID1 was mutated (R451Q) showed dramatically weakened binding to GST-LRP-CT (pY4507), while the binding of LRP-CT in the nonphosphorylated form was not affected. This effect was also observed using Fe65 WW-PID1. Also in agreement with the microdomain results, Fe65 PID2 binds preferentially to the nonphosphorylated form of LRP-CT (Figure 5C, lane 3).

Fe65 LRP-CT Binding Affinity Is in the Micromolar Range. To show specific, concentration-dependent binding of LRP-CT to Fe65 PID2, GST LRP-CT was incubated with varying amounts of Fe65 PID2 (536−662). GST LRP-CT bound more Fe65 PID2 when incubated with 24 μM Fe65 PID2 as compared to 12 μM Fe65 PID2 (Figure 5D).

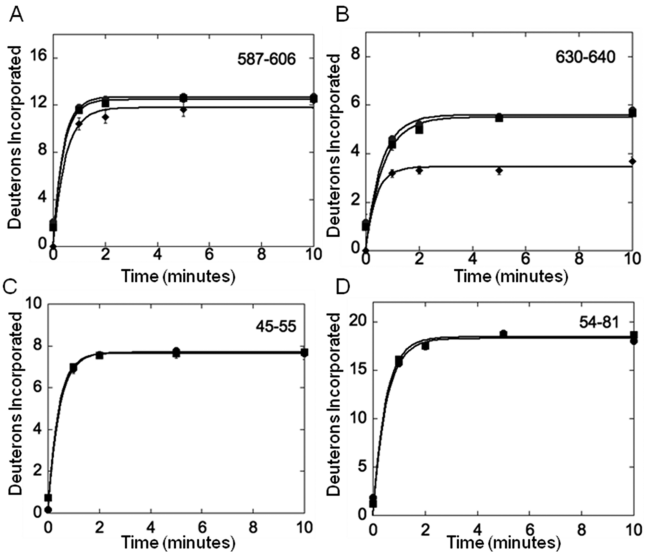

Figure 2. Plots of the amide H−D exchange of Fe65. (A) Deuterons incorporated over 10 min for Fe65 (1−662) (●), Fe65 (236−662) (■), and Fe65 (236−662) with AICD bound (◆). Residues 587−606 of PID2 are depicted and show the same solvent accessibility with or without the N-terminal domain. Fe65 (236−662) with AICD bound also showed the same solvent accessibility because this region is not in the Fe65−AICD binding interface. (B) Deuterons incorporated over 10 min for Fe65 (1−662) (●), Fe65 (236−662) (■), and Fe65 (236−662) with AICD bound (◆). Residues 630−640 of PID2 are depicted and show the same solvent accessibility with or without the N-terminal domain. Fe65 (236−662) with AICD bound showed decreased solvent accessibility for this region because it is in the binding interface. (C) Plots of the amide H−D exchange of Fe65 (236−662) (●) and Fe65 (236−512) (■) over 10 min. Residues 45−55 of the WW domain are depicted and showed the same solvent accessibility with or without PID2. (D) Plots of the amide H−D exchange of Fe65 (236−662) (●) and Fe65 (236−512) (■) over 10 min. Residues 54−81 of the WW domain are depicted and showed the same solvent accessibility with or without PID2.

To further establish the interaction between LRP-CT and Fe65, a truncated LRP-CT starting at position 4488 and ending at position 4454 (LRP4488) was attached through an N-terminal cysteine to Oregon Green 488 maleimide (Invitrogen) and used in fluorescence anisotropy binding studies. LRP4488 or pYLRP4488 was incubated with varying concentrations of Fe65 WW-PID1-PID2 (236−662) or WW-PID1 (236−512), and the fluorescence anisotropy change upon binding was measured (Figure 6). Both WW-PID1-PID2 and WW-PID1 showed preferred binding to pYLRP4488 with K_D values of 48.3 ± 7.3 and 66.7 ± 6.2 μM, respectively. Although nonphosphorylated LRP4488 appears to be weakly binding, the affinity was too weak to quantify.

LRP-CT and AICD Compete for Binding to Fe65 PID2. Both nonphosphorylated LRP-CT and AICD bind Fe65 PID2. To determine if these Fe65 ligands share the same binding site, we performed a competition binding experiment. GST-LRP-CT was immobilized on glutathione Sepharose and incubated with Fe65 PID2 (536−662) in the presence and absence of AICD. GST-LRP-CT bound significantly less Fe65 PID2 when an equimolar amount of AICD was present (in Figure 7, compare lanes 3 and 4).

Fe65 Binds Preferentially to LRP-CT Phosphorylated at Tyrosine 4507 When in Complex with AICD. Fe65 has been shown to form a trimeric complex with LRP-CT and AICD.[23] We tested whether the phosphorylation state of LRP-CT Y4507 affects the formation of this complex. Immobilized AICD was used as bait to capture purified Fe65 WW-PID1-PID2 (236−662) and LRP-CT or LRP-CT (pY4507). Fe65 and AICD preferentially form a complex with LRP-CT (pY4507) (Figure 8), but not the R451Q mutant, showing that LRP-CT (pY4507) is predominantly interacting with PID1 in the trimeric complex.

Table 2. Amide H−D Exchange

(A) Exchange into the PID2 Region of Fe65 (1−662) vs Fe65 (236−662)

Fe65 residue	peptide mass (Da)	no. of backbone amides	no. of amides exchanged after 5 min: Fe65 (1−662)	Fe65 (236−662)
565−589	2555.27	21	16.1 ± 0.1	16.2 ± 0.2
569−589	2127.05	18	12.7 ± 0.2	12.6 ± 0.2
603−610	924.54	6	2.5 ± 0.1	2.5 ± 0.2
610−621	1332.71	10	5.2 ± 0.1	5.3 ± 0.1
610−620	1185.64	9	5.5 ± 0.1	5.5 ± 0.2
638−649	1087.53	11	not determined	not determined

(B) Exchange into the WW Domain Region of Fe65 (236−702) vs Fe65 (236−512)

Fe65 residue	peptide mass (Da)	no. of backbone amides	no. of amides exchanged after 5 min: Fe65 (236−702)	Fe65 (236−512)
260−270	1320.59	10	7.8 ± 0.1	7.6 ± 0.2
269−296	3144.44	25	18.6 ± 0.1	18.8 ± 0.2

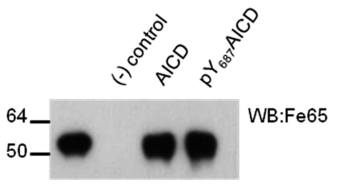

Figure 3. Dependence of binding of Fe65 to AICD on phosphorylation of AICD Y687 explored using immobilized AICD. AICD Y653F (GSKLCKKKQFTSIHHGVVEVDAAVTPEERHLSKMQQNGYENPTYKFFEQMQN) (5 μM) in the phosphorylated or nonphosphorylated form was immobilized using Sulfolink coupling gel and incubated with 180 nM Fe65 (236−662) for 1 h at 4 °C. Sulfolink resin alone was used as a negative control. Bound Fe65 was visualized by Western blotting with an anti-Fe65 antibody (1:500, Millipore, 3H6). Comparison of the third and fourth lanes reveals that Fe65 binds AICD in a manner independent of phosphorylation at Tyr687.

■ DISCUSSION

Fe65 contains three protein interaction domains, a WW domain followed by two PIDs. In addition to these defined domains, Fe65 contains an N-terminal region that has been proposed to inhibit interactions with Fe65 ligands.[17,18] Our SPR studies of AICD binding to Fe65 with and without the N-terminal region quantitatively show that the N-terminal region does indeed weaken binding of Fe65 PID2 to AICD, in agreement with the previous studies. It appears that effects from both the far

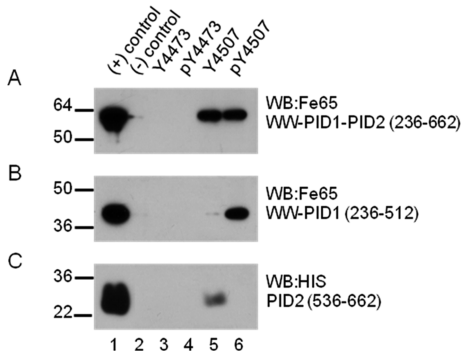

Figure 4. LRP-CT microdomains binding to (A) Fe65 WW-PID1-PID2 (236−662), (B) Fe65 WW-PID1 (236−512), or (C) Fe65 PID2 (536−662). Microdomains containing Y4473 (Cys-amino aminohexanoic acid-VEIGNPTY$_{4473}$KMYEGGE) or Y4507 (Cys-amino aminohexanoic acid-TNFTNPVY$_{4507}$ATLY) in both tyrosine-phosphorylated and nonphosphorylated forms were immobilized using Sulfolink coupling gel. Each microdomain (60 μg) was incubated with 180−400 nM Fe65 for 1 h at 4 °C. Sulfolink resin alone was used as a negative control. Bound Fe65 was visualized by Western blotting with anti-Fe65 antibody (Millipore, 3H6) or anti-HIS antibody (Qiagen, Penta-His Ab). Fe65 WW-PID1-PID2 bound to both the phospho and non-phospho forms of the Y4507-containing microdomain of LRP. Panel B shows that only the phospho form binds to Fe65 PID1, and panel C shows that only the non-phospho form binds to Fe65 PID2.

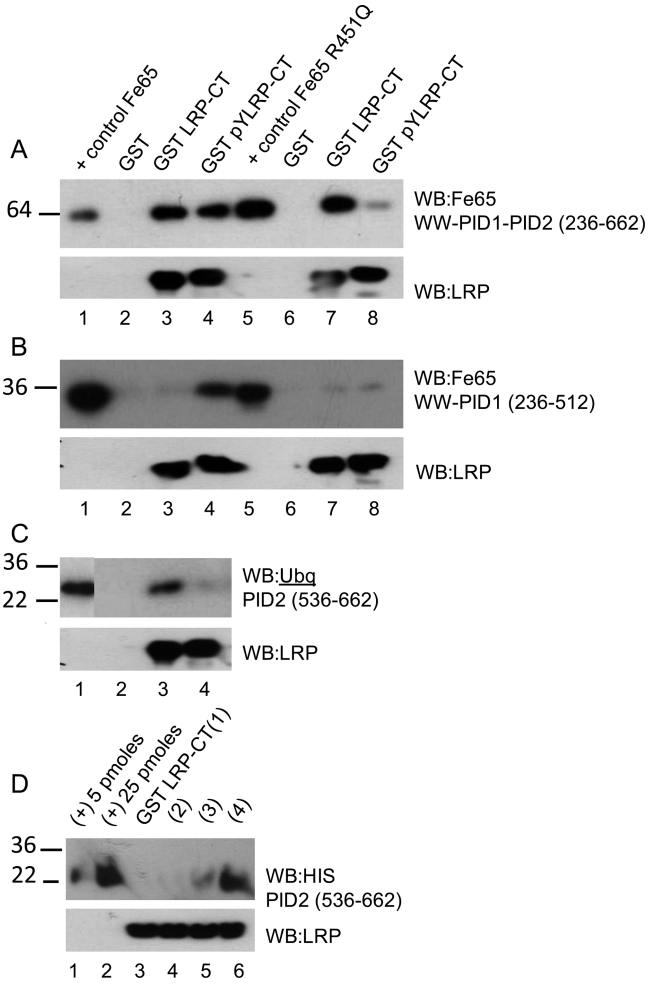

Figure 5. LRP-CT binding to (A) Fe65 WW-PID1-PID2 (236−662), (B) Fe65 WW-PID1 (236−512), or (C) Fe65 PID2 (536−662). GST-LRP-CT or GST-LRP-CT (pY4507) was immobilized on glutathione Sepharose and incubated at 650 nM with each Fe65 construct (lanes 2−4) or Fe65(R451Q) construct (lanes 6−8) at 180−400 nM for 1 h at 4 °C. GST-coupled Sepharose was used as a negative control. Bound Fe65 or Fe65 R451Q was visualized by Western blotting with the anti-Fe65 antibody (Millipore, 3H6) or anti-ubiquitin antibody (Invitrogen, 13-1600). Each Fe65 variant (0.05 pmol) was analyzed as a positive control (lanes 1 and 5). Equal LRP-CT loading is shown by Western blotting with the anti-LRP antibody (11H4). (D) LRP-CT binding to Fe65 PID2 (536−662). GST-LRP-CT was immobilized on glutathione Sepharose at 650 nM and was incubated with 3 (1), 6 (2), 12 (3), or 24 μM PID2 (4) for 1 h at 4 °C. Bound Fe65 was visualized by Western blotting with the anti-HIS antibody (Qiagen, Penta-His Ab). Fe65 PID2 (5 and 25 pmol) is shown as a positive control. Equal LRP-CT loading is shown by Western blotting with the anti-LRP antibody (11H4).

N-terminus and the WW-PID1 region contribute to weakening the binding of AICD to Fe65 PID2. Although we attempted to use amide H−D exchange to observe the putative intramolecular interactions that might be weakening the binding of AICD to Fe65 PID2, no differences in exchange could be attributed to the presence of the N-terminal region. This indicates that either the intramolecular interactions are too weak to observe by this method or the interactions take place in regions not covered in the H−D exchange experiment. Clear changes in PID2 were observed upon addition of AICD, arguing that the first scenario is more likely to be the case. The weaker binding affinity of the Fe65s containing the N-terminal domains was primarily due to slower association rates, perhaps indicating that these domains sterically hinder binding.

Phosphorylation of AICD has been observed in brains of Alzheimer's disease patients at several sites, including Y687.[34] We report here that AICD can be phosphorylated at Y687 by Src kinase in vitro. Our results show that tyrosine phosphorylation of the AICD NPXY$_{687}$ motif does not affect the binding of AICD to Fe65. The Fe65 PID2−AICD interaction has a large binding interface that does not rely solely on the AICD NPXY binding motif.[11] However, it is interesting that the addition of the phosphate group to a residue at the interface does not have a significant effect on binding affinity.

LRP-CT contains two NPXY motifs that can both be tyrosine-phosphorylated. We found that the NPXY$_{4507}$ motif, but not the NPXY$_{4473}$ motif, bound to Fe65, agreeing with previous binding studies using rat brain lysate.[28] All Fe65 interactions occur at the second NPXY$_{4507}$ motif in both the tyrosine-phosphorylated and nonphosphorylated forms. Using both the LRP-CT microdomains and full-length LRP-CT, we showed that Fe65 PID1 binds to LRP-CT phosphorylated at Y4507, while Fe65 PID2 prefers nonphosphorylated LRP-CT. Furthermore, we demonstrated that LRP-CT and AICD cannot bind Fe65 PID2 simultaneously, as they compete for binding in pull-down assays. LRP-CT must be phosphorylated at Y4507 to form a trimeric complex with Fe65 and AICD, in which AICD binds Fe65 PID2 and LRP-CT (pY4507) binds Fe65 PID1. Although the binding affinities for Fe65−LRP-CT complexes could not be determined by SPR or ITC because of the weak nature of the interaction, fluorescence anisotropy experiments show that Fe65 WW-PID1-PID2 binds pYLRP4488 with a K_D of 48.3 ± 7.3 μM and Fe65 WW-PID1 binds pYLRP4488 with a K_D of 66.7 ± 6.2 μM. These experiments further demonstrate that the predominant Fe65−LRP-CT interaction occurs through PID1 of Fe65 and LRP-CT phosphorylated at Y4507.

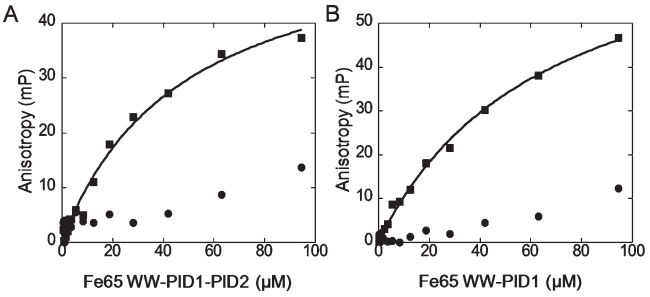

Figure 6. Fluorescence anisotropy of LRP4488 or pYLRP4488 binding to Fe65. LRP4488 (●) or pYLRP4488 (■) conjugated to Oregon Green 488 maleimide (Invitrogen) was incubated with 0.1−100 μM Fe65 WW-PID1-PID2 (236−662) (A) or 0.1−100 μM Fe65 WW-PID1 (236−512) (B). Anisotropy values at each Fe65 concentration were determined using a DTX 880 Multimode Dectector Beckman Coulter plate reader with an excitation filter at 485 nm and two emission filters at 535 nm equipped with polarizers. Data were fit with KaleidaGraph version 4.0 using a Michaelis−Menten curve fit. pYLRP4488 bound Fe65 WW-PID1-PID2 with a K_D of 48.3 ± 7.3 μM, and pYLRP4488 bound Fe65 WW-PID1 with a K_D of 66.7 ± 6.2 μM.

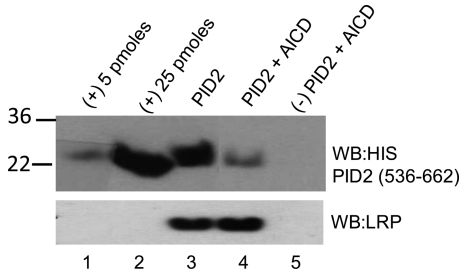

Figure 7. GST-LRP-CT (650 nM) was immobilized on glutathione Sepharose and allowed to bind 24 μM Fe65 PID2 (536−662) in the presence and absence of 650 nM AICD. GST-coupled Sepharose was used as a negative control. Bound Fe65 PID2 was visualized by Western blotting with the anti-HIS antibody (Qiagen, Penta-His Ab). Fe65 PID2 (5 and 25 pmol) is shown as a positive control. Equal LRP-CT loading is shown by Western blotting with the anti-LRP antibody (11H4).

Fe65 PID1 and PID2 have been classified as Dab-like PIDs on the basis of an algorithm using the structures of Dab1, Dab2, NUMB, and X11.[24] IRS-like PIDs were identified on the basis of the structures of IRS, Dok1, and Dok5, and no overlap was found between Dab-like and IRS-like identifications. On the other hand, the Dab-like algorithm identified 16 Shc-like family members showing these two families are close relatives. Although PID1 has been identified as a Dab-like PID, it contains features belonging to both the Shc-like and IRS-like PIDs. Shc-like PIDs contain an inserted 22-amino acid loop between α2 and β2, and Fe65 PID1 also contains a 19-amino acid insertion at this position. Structure and sequence alignments of Fe65 PID1 with the IRS-like PIDs reveal that Fe65 PID1 residues R451 and R470 correspond to the two key phosphate-coordinating arginine residues present in IRS-like PIDs (Figure 9). Remarkably, Fe65 PID1 binds exclusively to LRP-CT in the tyrosine-phosphorylated form, and the mutant Fe65 R451Q loses the ability to bind pYLRP-CT, consistent with the functional importance of these arginines. Thus, Fe65 PID1 is the first Dab-like PID demonstrated to have phosphorylation-dependent binding.

To explore other Dab-like PIDs that may also be phosphorylation-dependent, we used LALIGN to align Fe65 PID1 with all

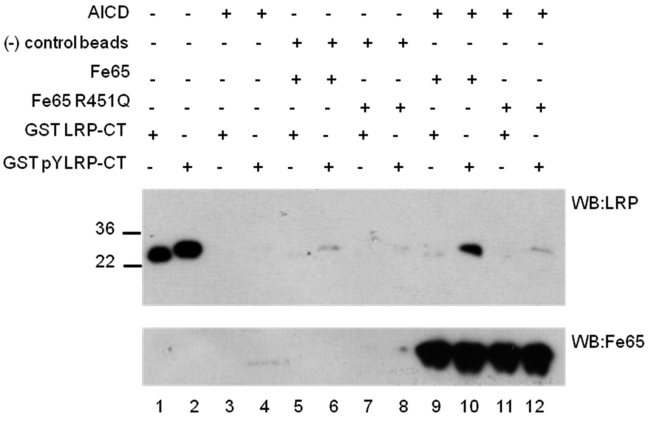

Figure 8. Phosphorylation-dependent binding of LRP-CT to Fe65 in the LRP-CT−Fe65−AICD trimeric complex was explored. Using Sulfolink coupling gel, 5 μM AICD was immobilized and incubated with 2.5 μM Fe65 WW-PID1-PID2 (236−662) and 260 nM GST-LRP-CT (pY4507) or GST-LRP-CT for 1 h at 4 °C. Sulfolink resin alone was used as a negative control to ensure LRP-CT was not detected because of aggregation. The reaction mixtures were washed and resuspended in reducing sample buffer. Bound GST-LRP-CT was visualized by Western blotting with the anti-LRP antibody (11H4). Equal Fe65 binding is shown by Western blotting with the anti-Fe65 antibody (Millipore, 3H6). GST-LRP-CT can form a complex with only Fe65 and AICD when phosphorylated at Y4507 (lane 10).

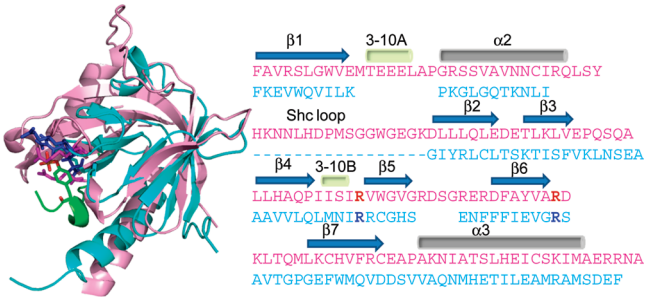

Figure 9. PyMol structural alignment of Fe65 PID1 (pink) (Protein Data Bank entry 3D8D[26]) with IRS PID (cyan) bound to the IL-4 receptor NPXY motif (green) (Protein Data Bank entry 1IRS[41]). The phosphotyrosine is colored according to the atoms; the conserved arginines in Fe65 PID1 are colored red and in IRS PID blue. Fe65 PID1 R451 and R470 align with the phosphate-coordinating arginines of IRS (R212 and R227) as shown in the sequence alignment presented with the same color scheme. The alignment was adapted from ref 26.

other Dab-like PIDs found by Unlik et al. in search of aligning the key arginine residues (R451 and R470). The Dab-like PIDs belonging to CAPON and GULP were found to have highly basic residues that aligned with the Fe65 PID1 arginine residues. CAPON has been shown to bind dexras and synapsin, neither of which contains an NPXY motif.[35,36] The PID of CAPON is not the only PID that has been shown to bind a ligand lacking an NPXY motif, demonstrating the high degree of variability in PID binding mechanisms.[37] PIDs, including that of Dab, have also been shown to bind phosphoinositide groups at a binding site distinct from the NPXY peptide binding groove.[38] The GULP PID has been shown to bind the NPXY motifs of LRP-CT, CED-1, and Stabilin-2.[39,40] Although these ligands contain NPXY motifs, they have all been shown to bind GULP in the nonphosphorylated form. It will be interesting to see whether

GULP will bind more strongly to pYLRP-CT. Our Dab-like PID search did not uncover any additional phosphorylation-dependent domains. We suspect that as the PID−ligand structure database is expanded, additional binding modes will be revealed and the PID classification system may need to be revised.

■ ASSOCIATED CONTENT

Supporting Information. An additional figure showing the purity of the proteins. This material is available free of charge via the Internet at http://pubs.acs.org.

■ AUTHOR INFORMATION

Corresponding Author

*Department of Chemistry and Biochemistry, University of California, San Diego, La Jolla, CA 92093-0378. Phone: (858) 534-3058. Fax: (858) 534-6174. E-mail: ekomives@ucsd.edu.

Present Addresses

†University of Washington, Medicinal Chemistry Health Sciences Building, Room H-172J, Seattle, WA 98195.

Funding Sources

Financial support for this work was provided by National Institutes of Health Grant RO1-AG025343 to E.A.K. M.M. was supported by the Hemoglobin and Blood Proteins Training Program (5T32DK007233).

■ ABBREVIATIONS

LRP, low-density lipoprotein receptor-related protein 1; APP, amyloid precursor protein; AICD, APP intracellular domain; CTF, C-terminal fragment; PID, protein interaction domain; ITC, isothermal titration calorimetry; HDX, hydrogen−deuterium exchange mass spectrometry; TFA, trifluoroacetic acid; ACN, acetonitrile.

■ REFERENCES

(1) Ulery, P. G., Beers, J., Mikhailenko, I., Tanzi, R. E., Rebeck, G. W., Hyman, B. T., and Strickland, D. K. (2000) Modulation of β-amyloid precursor protein processing by the low density lipoprotein receptor-related protein (LRP). Evidence that LRP contributes to the pathogenesis of Alzheimer's disease. *J. Biol. Chem. 275*, 7410–7415.

(2) Ando, K., Iijima, K. I., Elliott, J. I., Kirino, Y., and Suzuki, T. (2001) Phosphorylation-dependent regulation of the interaction of amyloid precursor protein with Fe65 affects the production of β-amyloid. *J. Biol. Chem. 276*, 40353–40361.

(3) Pietrzik, C. U., Busse, T., Merriam, D. E., Weggen, S., and Koo, E. H. (2002) The cytoplasmic domain of the LDL receptor-related protein regulates multiple steps in APP processing. *EMBO J. 21*, 5691–5700.

(4) Wang, B., Hu, Q., Hearn, M. G., Shimizu, K., Ware, C. B., Liggitt, D. H., Jin, L. W., Cool, B. H., Storm, D. R., and Martin, G. M. (2004) Isoform-specific knockout of FE65 leads to impaired learning and memory. *J. Neurosci. Res. 75*, 12–24.

(5) Zerbinatti, C. V., Wozniak, D. F., Cirrito, J., Cam, J. A., Osaka, H., Bales, K. R., Zhuo, M., Paul, S. M., Holtzman, D. M., and Bu, G. (2004) Increased soluble amyloid-β peptide and memory deficits in amyloid model mice overexpressing the low-density lipoprotein receptor-related protein. *Proc. Natl. Acad. Sci. U.S.A. 101*, 1075–1080.

(6) Santiard-Baron, D., Langui, D., Delehedde, M., Delatour, B., Schombert, B., Touchet, N., Tremp, G., Paul, M. F., Blanchard, V., Sergeant, N., Delacourte, A., Duyckaerts, C., Pradier, L., and Mercken, L. (2005) Expression of human FE65 in amyloid precursor protein transgenic mice is associated with a reduction in β-amyloid load. *J. Neurochem. 93*, 330–338.

(7) Hoe, H. S., Magill, L. A., Guenette, S., Fu, Z., Vicini, S., and Rebeck, G. W. (2006) FE65 interaction with the ApoE receptor ApoEr2. *J. Biol. Chem. 281*, 24521–24530.

(8) Smith, M. J., Hardy, W. R., Murphy, J. M., Jones, N., and Pawson, T. (2006) Screening for PTB domain binding partners and ligand specificity using proteome-derived NPXY peptide arrays. *Mol. Cell. Biol. 26*, 8461–8474.

(9) Zhang, Z., Lee, C. H., Mandiyan, V., Borg, J. P., Margolis, B., Schlessinger, J., and Kuriyan, J. (1997) Sequence-specific recognition of the internalization motif of the Alzheimer's amyloid precursor protein by the X11 PTB domain. *EMBO J. 16*, 6141–6150.

(10) Yun, M., Keshvara, L., Park, C. G., Zhang, Y. M., Dickerson, J. B., Zheng, J., Rock, C. O., Curran, T., and Park, H. W. (2003) Crystal structures of the Dab homology domains of mouse disabled 1 and 2. *J. Biol. Chem. 278*, 36572–36581.

(11) Radzimanowski, J., Simon, B., Sattler, M., Beyreuther, K., Sinning, I., and Wild, K. (2008) Structure of the intracellular domain of the amyloid precursor protein in complex with Fe65-PTB2. *EMBO Rep. 9*, 1134–1140.

(12) Boucher, P., Liu, P., Gotthardt, M., Hiesberger, T., Anderson, R. G., and Herz, J. (2002) Platelet-derived growth factor mediates tyrosine phosphorylation of the cytoplasmic domain of the low density lipoprotein receptor-related protein in caveolae. *J. Biol. Chem. 277*, 15507–15513.

(13) Betts, G. N., van der Geer, P., and Komives, E. A. (2008) Structural and functional consequences of tyrosine phosphorylation in the LRP1 cytoplasmic domain. *J. Biol. Chem. 283*, 15656–15664.

(14) Hu, Q., Cool, B., Wang, B., Hearn, M., and Martin, G. (2002) A candidate molecular mechanism for the association of an intronic polymorphism of FE65 with resistance to very late onset dementia of the Alzheimer type. *Hum. Mol. Genet. 11*, 465–475.

(15) Fiore, F., Zambrano, N., Minopoli, G., Donini, V., Duilio, A., and Russo, T. (1995) The regions of the Fe65 protein homologous to the phosphotyrosine interaction/phosphotyrosine binding domain of Shc bind the intracellular domain of the Alzheimer's amyloid precursor protein. *J. Biol. Chem. 270*, 30853–30856.

(16) Borg, J. P., Ooi, J., Levy, E., and Margolis, B. (1996) The phosphotyrosine interaction domains of X11 and FE65 bind to distinct sites on the YENPTY motif of amyloid precursor protein. *Mol. Cell. Biol. 16*, 6229–6241.

(17) Hu, Q., Wang, L., Yang, Z., Cool, B. H., Zitnik, G., and Martin, G. M. (2005) Endoproteolytic cleavage of FE65 converts the adaptor protein to a potent suppressor of the sAPPα pathway in primates. *J. Biol. Chem. 280*, 12548–12558.

(18) Cao, X., and Sudhof, T. C. (2004) Dissection of Amyloid-B Precursor Protein-dependent Transcriptional Transavtivation. *J. Biol. Chem. 279*, 24601–24611.

(19) Trommsdorff, M., Borg, J. P., Margolis, B., and Herz, J. (1998) Interaction of cytosolic adaptor proteins with neuronal apolipoprotein E receptors and the amyloid precursor protein. *J. Biol. Chem. 273*, 33556–33560.

(20) Zambrano, N., Minopoli, G., de Candia, P., and Russo, T. (1998) The Fe65 adaptor protein interacts through its PID1 domain with the transcription factor CP2/LSF/LBP1. *J. Biol. Chem. 273*, 20128–20133.

(21) Cao, X., and Sudhof, T. C. (2001) A transcriptionally active complex of APP with Fe65 and histone acetyltransferase Tip60. *Science 293*, 115–120.

(22) Kinoshita, A., Whelan, C. M., Smith, C. J., Mikhailenko, I., Rebeck, G. W., Strickland, D. K., and Hyman, B. T. (2001) Demonstration by fluorescence resonance energy transfer of two sites of interaction between the low-density lipoprotein receptor-related protein and the amyloid precursor protein: Role of the intracellular adapter protein Fe65. *J. Neurosci. 21*, 8354–8361.

(23) Pietrzik, C. U., Yoon, I. S., Jaeger, S., Busse, T., Weggen, S., and Koo, E. H. (2004) FE65 constitutes the functional link between the low-density lipoprotein receptor-related protein and the amyloid precursor protein. *J. Neurosci. 24*, 4259–4265.

(24) Uhlik, M. T., Temple, B., Bencharit, S., Kimple, A. J., Siderovski, D. P., and Johnson, G. L. (2005) Structural and evolutionary division of phosphotyrosine binding (PTB) domains. *J. Mol. Biol. 345*, 1–20.

(25) Eck, M. J., Dhe-Paganon, S., Trub, T., Nolte, R. T., and Shoelson, S. E. (1996) Structure of the IRS-1 PTB domain bound to the juxtamembrane region of the insulin receptor. *Cell 85*, 695–705.

(26) Radzimanowski, J., Ravaud, S., Schlesinger, S., Koch, J., Beyreuther, K., Sinning, I., and Wild, K. (2008) Crystal structure of the human Fe65-PTB1 domain. *J. Biol. Chem. 283*, 23113–23120.

(27) Guttman, M., Prieto, J. H., Croy, J. E., and Komives, E. A. (2010) Decoding of lipoprotein-receptor interactions: Properties of ligand binding modules governing interactions with apolipoprotein E. *Biochemistry 49*, 1207–1216.

(28) Guttman, M., Betts, G. N., Barnes, H., Ghassemian, M., van der Geer, P., and Komives, E. A. (2009) Interactions of the NPXY microdomains of the low density lipoprotein receptor-related protein 1. *Proteomics 9*, 5016–5028.

(29) Seeliger, M. A., Young, M., Henderson, M. N., Pellicena, P., King, D. S., Falick, A. M., and Kuriyan, J. (2005) High yield bacterial expression of active c-Abl and c-Src tyrosine kinases. *Protein Sci. 14*, 3135–3139.

(30) Bergqvist, S., Croy, C. H., Kjaergaard, M., Huxford, T., Ghosh, G., and Komives, E. A. (2006) Thermodynamics reveal that helix four in the NLS of NF-κB p65 anchors IκBα, forming a very stable complex. *J. Mol. Biol. 360*, 421–434.

(31) Mandell, J. G., Falick, A. M., and Komives, E. A. (1998) Measurement of amide hydrogen exchange by MALDI-TOF mass spectrometry. *Anal. Chem. 70*, 3987–3995.

(32) Croy, C. H., Bergqvist, S., Huxford, T., Ghosh, G., and Komives, E. A. (2004) Biophysical characterization of the free IκBα ankyrin repeat domain in solution. *Protein Sci. 13*, 1767–1777.

(33) Barnes, H., Ackermann, E. J., and van der Geer, P. (2003) v-Src induces Shc binding to tyrosine 63 in the cytoplasmic domain of the LDL receptor-related protein 1. *Oncogene 22*, 3589–3597.

(34) Lee, M. S., Kao, S. C., Lemere, C. A., Xia, W., Tseng, H. C., Zhou, Y., Neve, R., Ahlijanian, M. K., and Tsai, L. H. (2003) APP processing is regulated by cytoplasmic phosphorylation. *J. Cell Biol. 163*, 83–95.

(35) Jaffrey, S. R., Benfenati, F., Snowman, A. M., Czernik, A. J., and Snyder, S. H. (2002) Neuronal nitric-oxide synthase localization mediated by a ternary complex with synapsin and CAPON. *Proc. Natl. Acad. Sci. U.S.A. 99*, 3199–3204.

(36) Fang, M., Jaffrey, S. R., Sawa, A., Ye, K., Luo, X., and Snyder, S. H. (2000) Dexras1: A G protein specifically coupled to neuronal nitric oxide synthase via CAPON. *Neuron 28*, 183–193.

(37) Xu, H., Lee, K. W., and Goldfarb, M. (1998) Novel recognition motif on fibroblast growth factor receptor mediates direct association and activation of SNT adapter proteins. *J. Biol. Chem. 273*, 17987–17990.

(38) Stolt, P. C., Vardar, D., and Blacklow, S. C. (2004) The dual-function disabled-1 PTB domain exhibits site independence in binding phosphoinositide and peptide ligands. *Biochemistry 43*, 10979–10987.

(39) Su, H. P., Nakada-Tsukui, K., Tosello-Trampont, A. C., Li, Y., Bu, G., Henson, P. M., and Ravichandran, K. S. (2002) Interaction of CED-6/GULP, an adapter protein involved in engulfment of apoptotic cells with CED-1 and CD91/low density lipoprotein receptor-related protein (LRP). *J. Biol. Chem. 277*, 11772–11779.

(40) Park, S. Y., Kang, K. B., Thapa, N., Kim, S. Y., Lee, S. J., and Kim, I. S. (2008) Requirement of adaptor protein GULP during stabilin-2-mediated cell corpse engulfment. *J. Biol. Chem. 283*, 10593–10600.

(41) Zhou, M. M., Huang, B., Olejniczak, E. T., Meadows, R. P., Shuker, S. B., Miyazaki, M., Trub, T., Shoelson, S. E., and Fesik, S. W. (1996) Structural basis for the IL-4 receptor phosphopeptide recognition by the IRS-1 PTB domain. *Nat. Struct. Mol. Biol. 3*, 388–393.